10A.7 Impact of Cloud-radiative Processes on Predecessor Rain Events

Omar A. Nava and Robert G. Fovell*

Department of Atmospheric and Oceanic Sciences, University of California, Los Angeles

Lance F. Bosart

Department of Atmospheric and Environmental Sciences, University at Albany/SUNY, Albany, New York

ABSTRACT

A series of idealized numerical simulations is conducted to examine the effects of cloud-radiative processes on the formation of predecessor rain events (PREs) during the extratropical transition of a tropical cyclone. The simulations are performed using an aquaplanet version of the Weather Research and Forecasting v.3.5.1 model with a straight jet. This study finds that cloud radiative forcing (CRF), the interaction of hydrometeors with longwave (LW) and shortwave (SW) radiation, produces a more robust PRE storm structure with stronger convective activity and wider bands of heavy rainfall. When CRF is ignored, non-convective PRE rainfall associated with the microphysics scheme is reduced by as much as 50%. It is hypothesized that cloud-radiative processes favorably modify the vertical thermal distribution of the PRE storm structure. Radiative warming in the lower atmosphere induces a deeper trough across the PRE region, resulting in stronger associated low-level convergence and implied vigorous ascent, especially in conjunction with low-level frontogenetical forcing along a baroclinic zone. This study emphasizes that cloud-radiative processes cannot be neglected and motivates further research on how radiation parameterizations and microphysical schemes influence the storm dynamics of high-impact weather phenomena such as predecessor rain events.

1. Introduction

The term predecessor rain event (PRE) was coined by Cote (2007) to describe coherent mesoscale rainstorms that occur well in advance of recurving tropical cyclones (TCs) and have a high potential to cause flooding and adverse societal impacts. PREs typically occur near a low-level baroclinic zone, beneath the equatorward entrance region of an upper-level jet streak, and in the presence of a low-level moisture advection from a TC (Cote 2007; Galarneau et al. 2010; Moore 2010). The forcing for ascent provided by the upper-level jet streak combined with the deep tropical moisture and low-level frontogenesis along the baroclinic zone, bring together the necessary ingredients for heavy rainfall (Doswell et al. 1996). Because PREs are sustained by deep tropical moisture, they often manifest themselves as persistent heavy rainbands and possess significant potential to cause extreme rainfall totals and high-impact flooding (Cote 2007). This aspect has been underscored most recently by high-impact flood-producing PREs associated with TC Erin (2007; Galarneau et al. 2010; Schumacher et al. 2011; Schumacher and Galarneau 2012) and TCs Ike and Lowell (2008; Bosart et al. 2012; Schumacher and Galarneau 2012).

This study investigates the effects of cloud-radiative-forcing (CRF), the interaction of hydrometeors with longwave (LW) and shortwave (SW) radiation, on PRE development via idealized modeling. The sensitivity of radiation to microphysics, owing to how hydrometeors in different schemes interacted with radiative processes, was the finding of Fovell et al. (2010a), who demonstrated that the motion and structural variation of TCs in their microphysics (MP) ensemble disappeared when clouds were made transparent to radiation. Because the interaction with LW and SW radiation is determined by a hydrometeor's effective size (e.g. Dudhia 1989), MP schemes differ with respect to the amount and relative distributions of cloud ice, snow, cloud droplets, etc. (Fovell et al. 2010b). Using "semi-idealized" simulations of the Hurricane Weather Research and Forecasting model (HWRF) and an axisymmetric model, Bu et al. (2014) further demonstrated that CRF enhanced convective activity in the TC outer core, leading to a wider eye, broader tangential wind field, and a stronger secondary circulation.

Because PREs share similar characteristics with TCs (e.g. low-level inflow, upper-level outflow, vertical potential vorticity (PV) structure, latent heat release, etc.), it is hypothesized that CRF will have a similar effect on PRE structure and strength, specifically with regard to

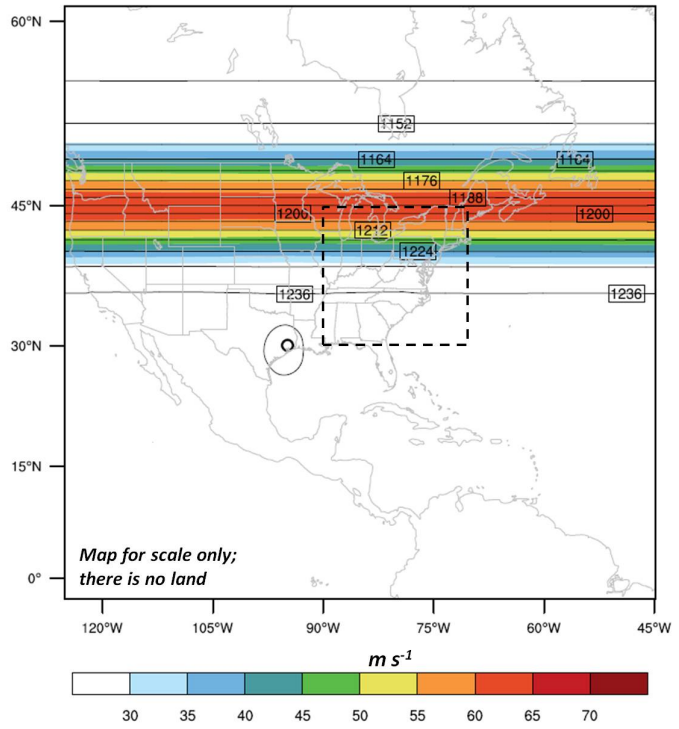

FIG. 1. Initial 200 hPa geopotential height (dam) and wind speed (colored) for the full simulation domain. The dashed black line indicates the analysis domain.

upward vertical motion resulting in enhanced precipitation.

2. Model and Experiment Design

An aquaplanet version of the Weather Research and Forecasting (WRF) model Advanced Research (ARW) core v.3.5.1 developed at the National Center for Atmospheric Research (NCAR) was selected for this study (Skamarock et al. 2008). The model setup is similar to the methodology of Fovell and Su (2007) who employed a modified real data version of the WRF model inspired by Hill and Lackmann (2009).

The simulation consisted of a single 9000 km square domain with 30 km horizontal resolution, 31 irregularly spaced vertical levels with a 50 mb model top, and was integrated over a period of 96 hours (Fig. 1). The MP scheme employed the five-class WRF single-moment (WSM5), which includes free-floating cloud droplets, rain, ice crystals, and slowly falling low-density aggregates (snow) (Hong et al. 2004). RRTMG (Rapid Radiative Transfer Model for General Circulation Models) was used for both LW and SW radiation (Iacono et al. 2008). CRF was controlled by the namelist parameter "icloud." When CRF is turned off, radiation is only affected by water vapor mixing ratio and transparent to clouds and all hydrometeors. In addition, the Kain-Fritsch (KF) convective parameterization, Yonsei University (YSU) boundary layer parameterization, and Noah Land Surface Model (LSM) were used.

An upper-tropospheric straight jet centered at 45°N with a maximum wind speed of 70 m s^{-1} at 175 hPa was generated following the methodology of Polvani et al. (2004). The corresponding mass and temperature fields were derived to be in geostrophic and hydrostatic balance with the vertical thermal and moisture profile specified by the Dunion (2011) moist tropical sounding. As in Ritchie and Elsberry (2001), a time-invariant sea surface temperature gradient is specified to match the near-surface air temperature gradient so that surface fluxes of moisture and heat do not erode the near-surface temperature structure through the simulation (not shown). South of the baroclinic zone, the SST was 26.8°C. In addition, because relative humidity is specified everywhere in the domain, the meridional temperature gradient implies moist (dry) air to the south (north). Initial experiments showed that the unperturbed jet remains stable throughout the 96-hour run, even including moist processes and sea surface fluxes (not shown).

To initiate the PRE, a TC with a maximum wind speed of 70 m s^{-1} located 40 km from the center was inserted south of the jet at 30°N using the TC bogusing initialization method introduced in WRF version 3 for cold start runs with background fields (Davis and Low-Nam 2001). The simulation was integrated initially for 48 hours with all parameterizations to develop a favorable environment for PRE initiation. Radiation effects were then modified and the simulation was integrated for the remaining 48 hours. Generally, PRE development began 51 hours into the simulation. This methodology minimized the effects of LW and SW radiation on the TC and environment, allowing for easier comparison of radiation effects on the PRE.

Cross-sections were calculated along a north-south longitude positioned approximately 1000 km to the northeast of the moving TC center, accordant with the average TC-PRE separation distance (Cote 2007; Galarneau et al. 2010). This provided a consistent reference point for comparison (see Fig. 2). The PRE cross-section was also averaged spatially across a 120 km longitude and temporally over a 6 hour period, allowing only persistent PRE features to manifest in the analysis.

3. Precipitation Field

Precipitation in the PRE region was initiated 51 hours into the simulation for both CRF-on and CRF-off cases. At 57 hours, precipitation began to differ significantly (not shown). PREs for both cases reached their peak intensity at 66 hours (Fig. 2), before decaying as the upper level

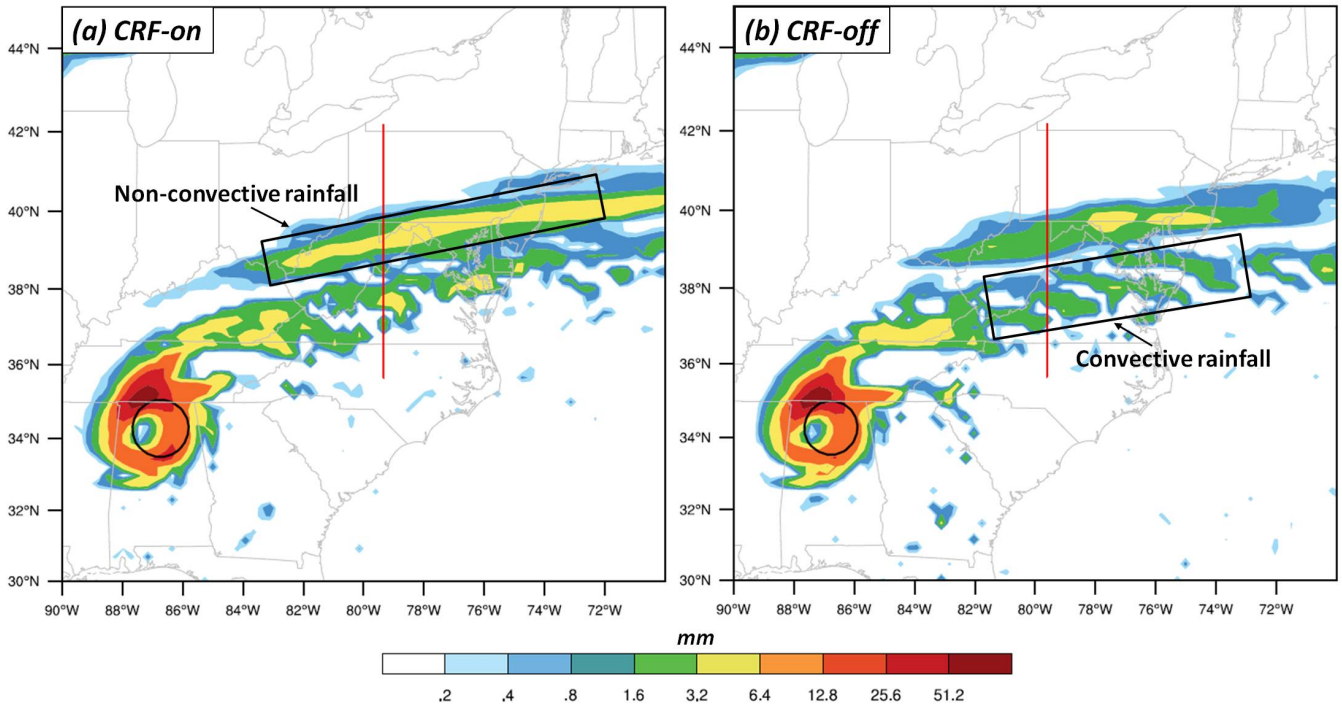

FIG. 2. 3-hour accumulated precipitation at 66 hours with (a) CRF-on and (b) CRF-off. The red line indicates the analysis cross-section. The black circle indicates the 986 hPa sea level pressure contour surrounding the TC center. Note the logarithmic scale.

jet maximum moved to the east (not shown). The largest rainfall differences were observed in the non-convective precipitation produced by the MP scheme, which was mainly located in the poleward half of the PRE region and characterized by a fairly coherent and uniform distribution (Fig. 2a). In general, the CRF-on case doubled the amount of non-convective rainfall produced by the CRF-off case. For convective precipitation, the effects of CRF were less dramatic. CRF-on produced slightly more rainfall, which was cellular in appearance and generally located equatorward of the main PRE precipitation band (Fig. 2b). Overall, the PRE lifecycle in these simulations was about 15 hours, which is consistent with the average PRE duration (Cote 2007; Galarneau et al. 2010).

In the semi-idealized simulations of Bu et al. (2014), CRF generated slow sustained ascent throughout the TC outer core which resulted in enhanced convective activity. The rainfall disparity in the PRE cases suggests that CRF produces a similar effect. For non-convective precipitation, increased vertical velocities lift more low-level moisture into the mid and upper atmosphere, enabling the MP scheme to produce more clouds, rain, and other hydrometeor species. Convective rainfall is also increased since the KF convective parameterization (CP) scheme uses low level vertical velocities as a "trigger" function to initiate deep convection and generate rainfall (Kain 2004).

4. PRE Vertical Wind Circulation

The upward vertical motions and wind circulations in the PRE structure due to CRF were investigated using time- and spatially-averaged vertical cross-sections relative to the TC center during the PRE mature stage at 66 hrs (Fig. 3). Similar to the methodology in Bu et al. (2014), the relative contribution of the cooling and warming on the PRE structure and dynamics associated with CRF was investigated. The "CRF $>$ 0" simulation only allowed the positive component of CRF to interact with the hydrometeor species, mainly resulting in warming confined to the cloudy area. Likewise, the "CRF $<$ 0" simulation isolated the negative component of CRF, which generally manifested as cooling at the cloud tops. The clear-sky forcing was permitted to vary with the diurnal cycle.

In comparison to the CRF-off case, CRF-on (Fig. 3a) shows increased low-level convergence and upward vertical motion from the surface to about 8.0 km, ending below the region of enhanced cooling along the cloud tops. Above 8.0 km, divergent upper-level wind flow supports the low-level upward motion and generates a wider PRE anvil (not shown). The enhanced vertical velocities in the PRE structure associated with CRF-on are congruous with the

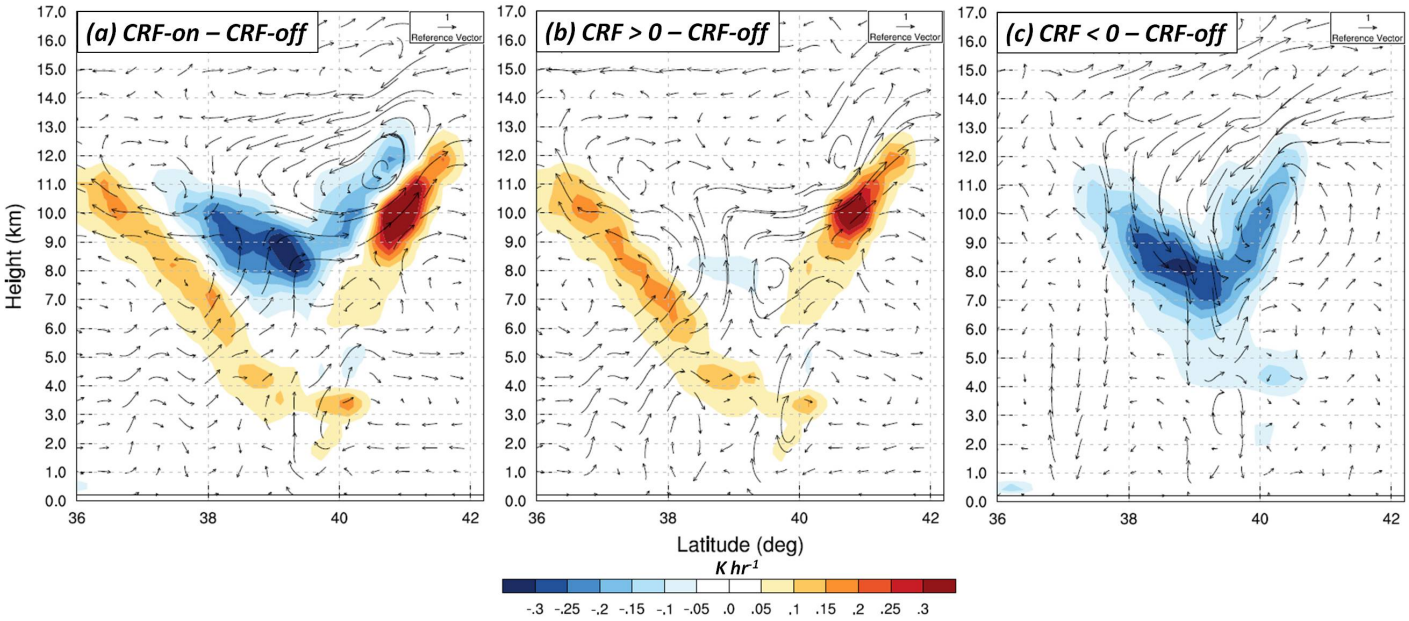

FIG. 3. Vertical cross-section of LW and SW radiation tendency difference (colored) and wind circulation difference for a) CRF-on - CRF-off, b) CRF > 0 - CRF-off, and c) CRF < 0 - CRF-off.

larger rainfall amounts noted in Figure 2. The CRF > 0 case (Fig. 3b) also shows increased low level convergence with an even deeper layer of upward vertical motion, extending from the surface through 9.0 km. The CRF > 0 case also indicates less downward vertical motion in the upper atmosphere that may hinder upward vertical motion from below. The small area of cooling in the center of the PRE structure is due to decreased clear-sky SW warming as a result of greater upper-level cloud cover in the CRF > 0 case (not shown). Conversely, the CRF < 0 case (Fig. 3c) generates relatively strong downward vertical motion in the upper atmosphere with almost no indication of upward vertical motion in the lower atmosphere.

Consistent with these results, the CRF > 0 case produced slightly more rainfall than CRF-on, while the CRF < 0 case generated slightly less rainfall than the CRF-off case (not shown). Because of upper-level downward vertical motion, cloud-top cooling does not contribute to PRE intensification and may even be a source of weakening. In agreement with previous findings, only the in-cloud warming generated by the interaction of LW radiative processes with hydrometeors enhances upward vertical motions in the PRE structure and, consequently, increases precipitation amounts Bu et al. (2014).

5. Horizontal Wind Circulation

CRF also induced a horizontal cyclonic circulation that helps enhanced upward vertical motion across the PRE region. CRF modifies the environmental temperature which is evident in the distribution of potential vorticity (PV). In the CRF-on case (Fig. 4a), there is positive PV anomaly tower in the lower atmosphere associated with the PRE. The local PV maximum around the freezing level is generated by latent heat release from condensation, freezing, and deposition processes captured by the MP scheme. The PV anomaly extends down to the surface as a result of convergence along the low-level baroclinic zone. Compared to the CRF-off case (Fig. 4b), CRF-on not only produces a slightly weaker PV tower but also generates an equatorward positive PV anomaly from the surface to about 4.0 km. This low-level PV anomaly "couplet" implies that CRF generates a cyclonic circulation in the lower atmosphere, resulting in enhanced eastward and westward winds centered on the equatorward positive PV anomaly (Fig. 4c).

The enhanced near-surface cyclonic circulation also suggests the presence of a low pressure trough generated by increased LW warming in the lower atmosphere associated with CRF (Fig. 5). Because of frictional effects in the boundary layer, the induced cyclonic circulation resulted in low-level convergence and enhanced upward vertical motion along the baroclinic zone. Consequently, this produced more convective and non-convective precipitation via the model CP and MP schemes, respectively. The deeper trough and stronger low-level circulation may also be responsible for the greater longitudinal extent of the PRE in the CRF-on case (Fig. 2a). While the CRF > 0

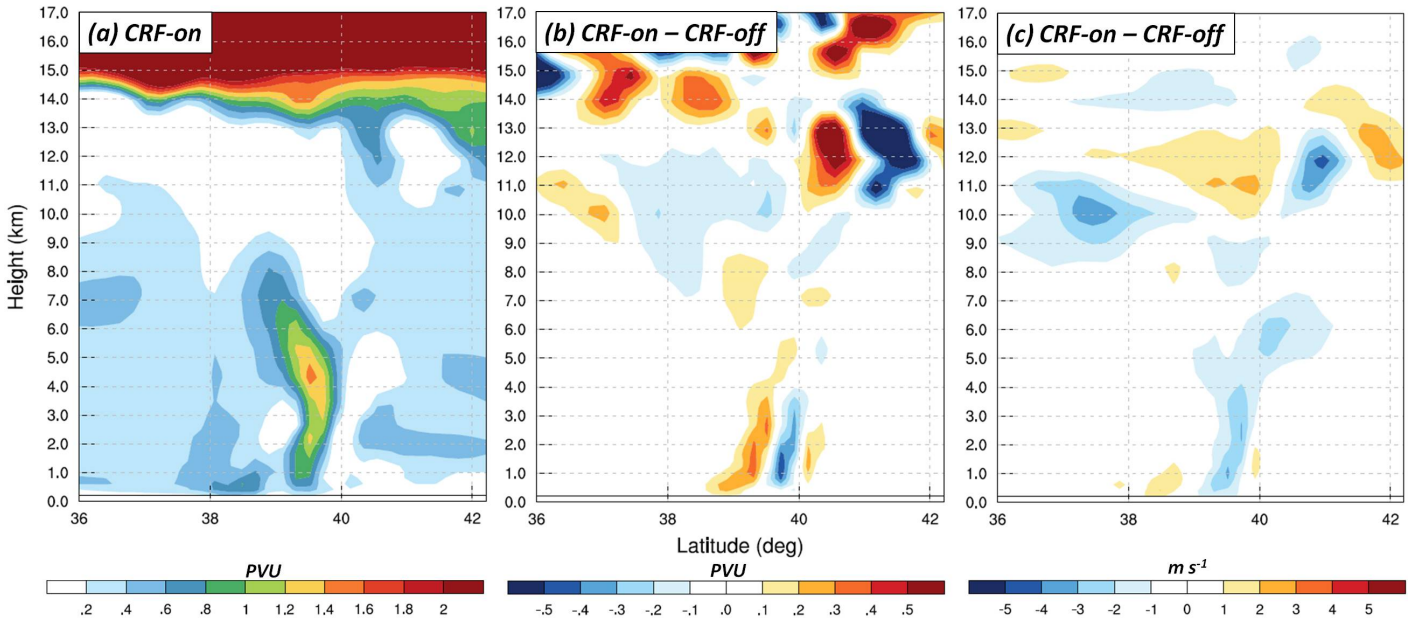

FIG. 4. Vertical cross-sections of a) PV with CRF-on, b) PV difference between CRF-on and CRF-off, and c) zonal wind difference between CRF-on and CRF-off. In panel (c), positive values indicate eastward zonal winds

case was almost identical to CRF-on, the CRF < 0 case did not produce a discernible low pressure trough across the PRE region (not shown), further highlighting the role of lower atmospheric warming in generating greater rainfall amounts.

6. Summary

This study represents a leading effort to examine the development and structure of PREs in an idealized modeling framework. The results support the findings of Bu et al. (2014) who investigated the effects of CRF on tropical cyclone structure using semi-idealized modeling. For PREs, CRF produced greater convective and non-convective precipitation as a result of enhanced upward vertical motion associated with lower atmospheric (primarily LW) warming. This generated a deeper trough with a broad low-level cyclonic circulation across the PRE region, resulting in stronger associated low-level convergence and more vigorous ascent, especially along the low-level baroclinic zone. Combined with latent heat release in the middle atmosphere, a positive feedback forms that enables PREs to intensify in a short period of time.

Even though this study mainly focused on PRE dynamics, CRF effects on the entire domain to include the TC cannot be ignored. CRF can strongly modulate the size and strength of the TC outer wind field, potentially influencing cyclone track (Bu et al. 2014; Fovell et al. 2010a). Since PRE development has been shown to occur relative to the position of the TC center (Cote 2007; Galarneau et al. 2010; Moore 2010), accurate forecasts of the TC track and intensity are critical to forecasting both locations and severity of PRE heavy rainfall.

Overall, the results of this study emphasize that cloud-radiative processes are important and motivates further research on how radiation parameterizations and microphysical schemes influence the storm dynamics of high-impact weather phenomena such as predecessor rain events.

REFERENCES

Bosart, L. F., J. M. Cordeira, T. J. Galarneau, Jr., B. J. Moore, and H. M. Archambault, 2012: An analysis of multiple predecessor rain events ahead of Tropical Cyclones Ike and Lowell: 10-15 September 2008. *Mon. Wea. Rev.*, **140 (4)**, 1081–1107.

Bu, Y. P., R. G. Fovell, and K. L. Corbosiero, 2014: Influence of cloud-radiative forcing on tropical cyclone structure. *J. Atmos. Sci.*, doi:10.1175/JAS-D-13-0265.1., in press.

Cote, M. R., 2007: Predecessor rain events in advance of tropical cyclones. M.S. thesis, Department of Atmospheric and Environmental Sciences, University at Albany, State University of New York, Albany, NY, 198 pp.

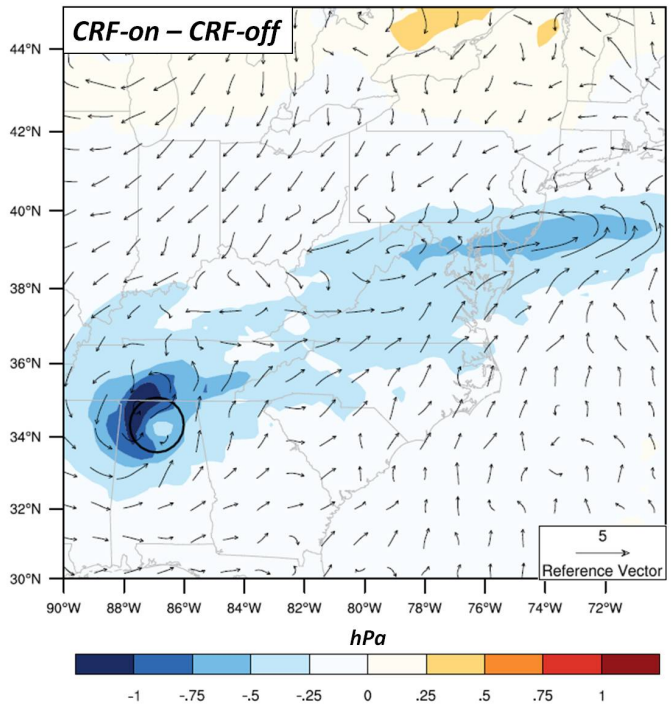

FIG. 5. 6-hour averaged 1 km pressure difference (colored) and wind difference between CRF-on and CRF-off.

Davis, C. A. and S. Low-Nam, 2001: The NCAR-AFWA tropical cyclone bogussing scheme. Tech. rep., Air Force Weather Agency (AFWA).

Doswell, C. A., III, H. E. Brooks, and R. A. Maddox, 1996: Flash flood forecasting: An ingredients-based methodology. *Wea. Forecasting*, **11**, 560–581.

Dudhia, J., 1989: Numerical study of convection observed during the winter monsoon experiment using a mesoscale two-dimensional model. *J. Atmos. Sci.*, **46 (20)**, 3077–3107.

Dunion, J. P., 2011: Rewriting the Climatology of the Tropical North Atlantic and Caribbean Sea Atmosphere. *J. Climate*, **24 (3)**.

Fovell, R. G., K. Corbosiero, and H. C. Kuo, 2010b: Influence of cloud-radiative feedback on tropical cyclone motion: Symmetric contributions. *29th Conf. on Hurricanes and Tropical Meteorology*, American Meteorological Society.

Fovell, R. G., K. L. Corbosiero., A. Seifert, and K. N. Liou, 2010a: Impact of cloud-radiative processes on hurricane track. *Geophys. Res. Lett.*, **37 (7)**, doi:10.1029/2010GL042691.

Fovell, R. G. and H. Su, 2007: Impact of cloud microphysics on hurricane track forecasts. *Geophys. Res. Lett.*, **134**, L24810, doi:10.1029/2007GL031723.

Galarneau, T. J., Jr., L. F. Bosart, and R. S. Schumacher, 2010: Predecessor rain events ahead of tropical cyclones. *Mon. Wea. Rev.*, **138 (8)**, 3272–3297.

Hill, K. A. and G. M. Lackmann, 2009: Influence of environmental humidity on tropical cyclone size. *Mon. Wea. Rev.*, **137 (10)**, 3294–3315, doi:10.1175/2009MWR2679.1.

Hong, S., , J. Dudhia, and S. Chen, 2004: A revised approach to ice microphysical processes for the bulk parameterization of clouds and precipitation. *Mon. Wea. Rev.*, **132 (1)**, 103–120.

Iacono, M. J., J. S. Delamere, E. J. Mlawer, M. W. Shephard, S. A. Clough, and W. D. Collins, 2008: Radiative forcing by long-lived greenhouse gases: Calculations with the AER radiative transfer models. *J. Geophys. Res.*, **113 (D13)**, D13 103, doi:10.1029/2008JD009944.

Kain, J., 2004: The Kain-Fritsch convective parameterization: an update. *J. Appl. Meteor. Climatol.*, **43 (1)**.

Moore, B. J., 2010: Synoptic-scale environments and dynamical mechanisms associated with predecessor rain events ahead of tropical cyclones. M.S. thesis, Department of Atmospheric and Environmental Sciences, University at Albany, State University of New York, Albany, NY, 150 pp.

Polvani, L. M., R. K. Scott, and S. J. Thomas, 2004: Numerically converged solutions of the global primitive equations for testing the dynamical core of atmospheric GCMs. *Mon. Wea. Rev.*, **132 (11)**, 2539–2552.

Ritchie, E. A. and R. L. Elsberry, 2001: Simulations of the transformation stage of the extratropical transition of tropical cyclones. *Mon. Wea. Rev.*, **129 (6)**, 1462–1480.

Schumacher, R. S. and T. J. Galarneau, Jr., 2012: Moisture transport into midlatitudes ahead of recurving tropical cyclones and its relevance in two predecessor rain events. *Mon. Wea. Rev.*, **140 (6)**, 1810–1827.

Schumacher, R. S., T. J. Galarneau, Jr., and L. F. Bosart, 2011: Distant effects of a recurving tropical cyclone on rainfall in a midlatitude convective system: a high-impact predecessor rain event. *Mon. Wea. Rev.*, **139 (2)**, 650–667.

Skamarock, W. C., J. Klemp, J. Dudhia, D. Gill, and D. M. Barker, 2008: A description of the Advanced Research WRF version 3. Ncar tech. note, Note NCAR/TN-4751STR.